The curves of Eduard Lehr

Péter Salvi

Budapest University of Technology and Economics



Abstract

The class of curves whose curvature is a trigonometric function of the arc length has appeared multiple times in the last century, in different contexts. It was first studied by Eduard Lehr, in a relatively obscure work. Due to renewed interest in it within the field of aesthetic curves, we summarize its most important results in this paper.

1. Introduction

Aesthetic plane curves are often defined by their Cesàro equation, i.e., the curvature as a function of arc length. A well-known example is the class of *log-aesthetic* curves,⁵ but a few other types are also briefly explored in Alfred Gray's textbook (Sections 5.3–5.4),¹ including one where

$$\kappa(s) = c \sin s,\tag{1}$$

with c being an arbitrary constant. This is quoted in Stephen Wolfram's A New Kind of Science (p. 418, example (j) in the figure),⁸ and the corresponding note on p. 1009 adds that the case of $\kappa(s) = a \sin(bs)$ 'was studied by Eduard Lehr in 1932'. Lehr's dissertation³ was already in Gray's bibliography, although no explicit reference was made there.

The curve in question, in slightly different form, has been used in geophysics to model river meandering since the 1960s,⁴ as it closely resembles the naturally occuring shape of *elastica*. There it is called a *sine-generated* curve, and it is defined by its tangent angle:

$$\theta(s) = \omega \sin \frac{2\pi s}{L}.\tag{2}$$

Here ω is the maximum turning angle and L is the total length. Deriving this we arrive at the Cesàro equation

$$\kappa(s) = \frac{2\pi\omega}{L}\cos\frac{2\pi s}{L}.$$
 (3)

Recently, the simplified formulation

$$\kappa(s) = \cos\frac{s}{c} \tag{4}$$

was proposed as an intrinsically fair curve representation, by the name *trig-aesthetic* curve (see Fig. 1).⁷

It appears that the first study of this class of curves was

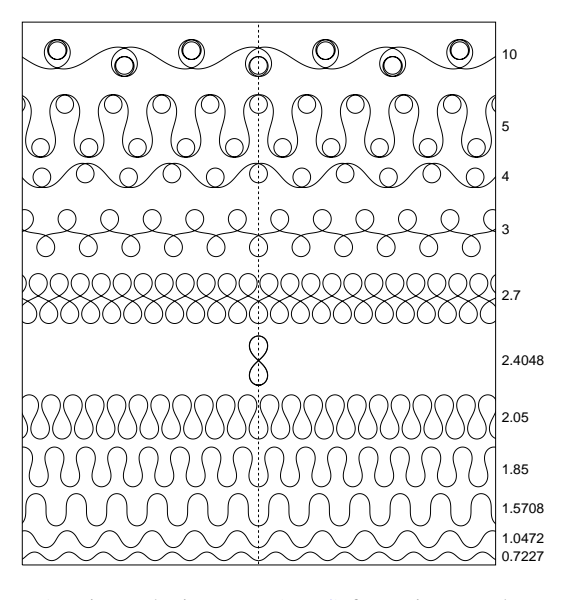


Figure 1: Trig-aesthetic curves (Eq. 4) for various c values. The s=0 points are always placed on the dotted line.

carried out by Lehr, but his work is in German, and it is available only in a handful of libraries. This paper aims to summarize his most important results.

2. Who was Eduard Lehr?

Eduard Lehr was born in 25 July 1906, in Ingolstadt, to Franz Xavier Lehr, a senior teacher and headmaster in Munich. He studied to be a teacher and passed the examinations in 1929–30, while also working as an assistant for descriptive geometry at the Technical University of Munich (then



Figure 2: Excerpt from the military records on Eduard Lehr.

still called *Technische Hochschule München*). He wrote his dissertation there in 1932, first under the "father of glacier photogrammetry", Sebastian Finsterwalder, then—after his advisor's retirement—under Josef Lense (known from the Lense–Thirring effect).[†]

He started his military training in 1936, and did military service during the Second World War with various antiaircraft artillery batallions in Nuremberg, Darmstadt and other places, eventually rising to the rank of first lieutenant of the reserve. According to the assessments in his military records (see Fig. 2), he was a slender man of small build, quiet and earnest, somewhat shy, but possessed a strong will. He lacked leadership skills, however, and in 1941, upon being appointed commander of a coastal battery, he suffered a nervous breakdown and requested a transfer to the weather service.

In 1942 he married Barbara Horras, the daughter of a locomotive driver, but she died pregnant in an air raid in 1945, leaving Lehr a childless widower. After the war, he was briefly suspended from teaching due to his membership in the Nazi Party and other pro-nazi organizations. Classified as a minor offender, he was reinstated in 1947; he taught mathematics and physics in Traunstein and later in Munich. His last workplace was the Max-Planck-Gymnasium, where he also acted as director from 1952 until his untimely death in 1955 (see Fig. 3).

Apart from his dissertation, only one other scientific work is attributed to him, although we have not been able to locate it: "Über die Dreiecksteilung von Vieleckern durch Ecktransversalen" (On the triangulation of polygons using vertex transversals).

3. Lehr's curves

The dissertation of Eduard Lehr bears the title 'On curves whose curvature is a periodic function of arc length' (Fig. 4).



Figure 3: A photo of Eduard Lehr from his obituary at the Max-Planck-Gymnasium München.

It is dedicated to the analysis of the curve family defined by the intrinsic equation

$$\kappa = \frac{1}{\rho} = a + b\cos(cs). \tag{5}$$

Note the presence of the additional term a, which—as we will see below—adds many different shapes to those in Equations (1) or (4). In the following, we will distinguish the shape parameter of trig-aesthetic curves (Eq. 4) with a hat (\hat{c}) to differentiate it from the c parameter in Eq. (5).

In the rest of this section, we will go through the main results of Lehr's work, following largely its original structure.

3.1. General properties

We can assume without loss of generality that $a \ge 0$, b > 0 and c > 0 (the b = 0 and c = 0 cases are just circles). Due to the symmetric shape of the cosine function, it is enough to examine a half period of the curve, starting from $s_0 = 0$ and ending in $s_1 = \frac{\pi}{c}$. All symbols with indices 0 and 1 relate to these endpoints, e.g. θ_0 is the starting tangent angle. The points themselves are denoted by P_0 and P_1 . Symbols with a bar (e.g. \bar{s}) are associated with the inflection point.

Since $\rho \neq 0$ there are no cusps, and the curvature extrema are in the endpoints. We only have an inflection when $a \leq b$ (which is actually just a flat point when a = b). The endpoints are the only vertices (i.e., points where $d\kappa/ds = 0$).

[†] https://mathgenealogy.org/id.php?id=65765

[‡] Notations are as in Lehr's work, except for θ and ϕ , which have their roles reversed. Additionally, curvature (κ) is often used, while only the radius of curvature (ρ) is seen in the original.

Überdie Kurven, deren Krümmung eine periodische Funktion des Bogens ist.

Von der Technischen Hochschule München zur Erlangung der Würde eines Doktors der technischen Wissenschaften genehmigte Abhandlung.

> Vorgelegt von Studienassessor Eduard Lehr, geboren zu Ingolstadt

Berichterstatter:
 O. Prof. Geh. Rat Dr. rer. nat. Dr. Dr. d. techn. Wissensch. eh.
 Dr. phil. eh. Sebastian Finsterwalder.
 2. Berichterstatter:
 O. Prof. Dr. phil. Joseph Lense.

Tag der Einreichung der Arbeit: 21. I. 1932. Tag der Annahme der Arbeit: 24. II. 1932.

Figure 4: The cover page of Eduard Lehr's dissertation.

The shape is defined by the ratio a:b:c, so we have only 2 degrees of freedom if we do not care about the scaling. A simple convention is to fix $\kappa_0=a+b=1$. To exclude rotations we will also assume $\theta_0=0$, so

$$\theta = as + \frac{b}{d}\sin(cs)$$
 \Rightarrow $\theta_1 = \frac{a\pi}{c}$. (6)

Consequently, when $\frac{a}{c}$ is an integer, the tangents at the endpoints are parallel. If in addition P_1 is on the normal line of P_0 the curve is closed. When $\frac{a}{c}$ is not an integer, the whole periodic curve remains inside a circle around M, where M is the intersection of the normals at the endpoints. It becomes a closed curve only when

$$\theta_1 = m\pi + \frac{v}{n}\pi,\tag{7}$$

where m, n and v are integers, v and n are relative prime, and v < n. In this case, the curve will make n periods and v full turns until it closes in itself, making m extra loops at the vertices. (See also Section 3.5 and Appendix A.)

We also define the excess angle as

$$\phi = \bar{\theta} - \theta_1 = \frac{1}{c} \left(\sqrt{b^2 - a^2} - a \arccos \frac{a}{b} \right). \tag{8}$$

Note that ϕ is imaginary for a > b. Lehr regards the $\phi = 0$ (i.e., a = b), $\theta_1 > 0$ case as the *base form*; other notable forms are (i) the *intermediary forms*, when $\theta_1 > 0$ and $0 < |\phi| < \infty$ (i.e., $0 \neq a \neq b \neq 0$), and (ii) that which are now

called *trig-aesthetic* curves (cf. Eq. 4), when a = 0. All other cases are either circles or straight lines.

3.2. Related curves

Here we examine some derived curve expressions.

3.2.1. Evolute

Following Cesàro 2 (Section II, Eq. 13), Lehr defines a series of radii of curvature as §

$$\rho_{(0)} = \rho, \qquad \qquad \rho_{(k)} = \rho \frac{d}{ds} \rho_{(k-1)}.$$
(9)

Then the arc length of the evolute is $s' = \rho$, its radius of curvature is $\rho' = \rho_{(1)}$; the tangent angle is the same as of the original curve, i.e., $\theta' = \theta$. Consequently, the evolute has cusps at the endpoints.

The differential equation form of our curves is

$$\rho_{(1)}^2 = c^2 \rho^4 (b^2 \rho^2 - (1 - a\rho)^2), \tag{10}$$

from which the intrinsic equation of the evolute is

$$\rho'^{2} = c^{2} s'^{4} (b^{2} s'^{2} - (1 - as')^{2}). \tag{11}$$

3.2.2. Offset

The curve at distance p has arc length $S = s + p\theta$, radius of curvature $R = \rho + p$, and tangent angle $\Theta = \theta$. Since $\rho = -p$ implies a zero radius of curvature, there will be a cusp there, except when it coincides with the endpoint.

We can express our curve based on its offset:

$$S = \frac{p}{c} \sqrt{b^2 - \left(\frac{1}{R - p} - a\right)^2} + \frac{1 + ap}{c} \arccos \frac{\frac{1}{R - p} - a}{b},$$
(12)

which becomes purely algebraic in the case of $p = -\frac{1}{a}$:

$$(aR+1)^{2}(a^{2}c^{2}S^{2}-b^{2})+a^{4}R^{2}=0.$$
 (13)

The intrinsic equation of the offset (from Eq. 10) is

$$P^{2} = c^{2}(R-p)^{4}(b^{2}(R-p)^{2} - (1+ap-aR)^{2}).$$
 (14)

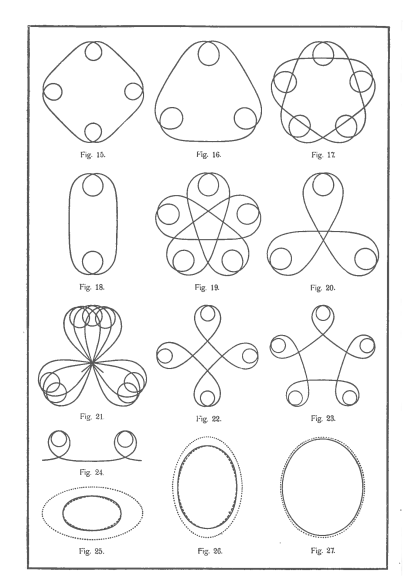
The meaning of P is not discussed, but it is evidently

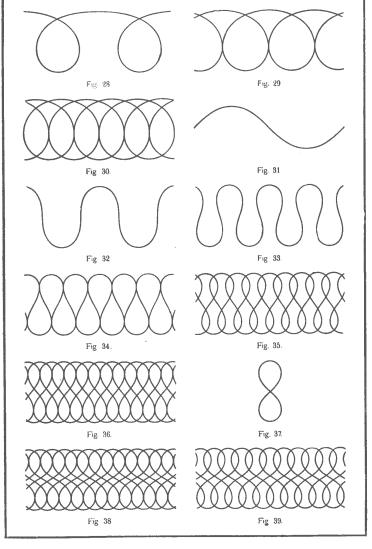
$$P = \rho_{(1)} = R \cdot \frac{\mathrm{d}R}{\mathrm{d}S}.\tag{15}$$

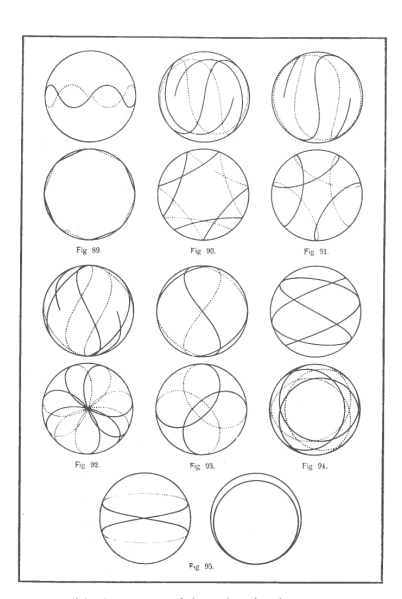
3.2.3. Involute

The involute has radius of curvature R' = s + p', and the derivative of its arc length (w.r.t. the arc length of the original curve) is $dS'/ds = R'\kappa$. Here p' is the initial length of 'unwrapped string'. Although there is always a point where R' = 0, there are no cusps, vertices or inflections.

 $[\]S$ Here we also deviate slightly from Lehr's notation, who uses $\rho', \rho'', \rho''', \dots$ for the series of radii of curvature.







(a) Two pages with planar curves

(b) A page with spherical curves

Figure 5: Curves drawn by Eduard Lehr.

Setting the starting parameter at the common point, the intrinsic equation for the involute is

$$2cS' = ac^{2}R'^{2} + 2b(cR'\sin(c(R'-p')) + \cos(c(R'-p')) - \cos(cp')).$$
 (16)

3.3. Invariants

In his seminal work on intrinsic equations (Section IV/8), Cesàro² defines the *invariant* of a curve family as a function of the first k radii of curvature that is constant zero. In the general case, the invariant for our curves is

$$\begin{split} \rho^{3}(\rho_{(1)}\rho_{(4)}-\rho_{(2)}\rho_{(3)}) - 12\rho^{2}\rho_{(1)}^{2}\rho_{(3)} + \\ & 60\rho_{(1)}^{3}(\rho\rho_{(2)}-\rho_{(1)}^{2}). \end{split} \tag{17}$$

When a = b we get a simpler expression:

$$\rho^{2}\rho_{(3)} - 8\rho\rho_{(1)}\rho_{(2)} + 10\rho_{(1)}^{3}, \tag{18}$$

and also for the a = 0 case:

$$\rho^2 \rho_{(3)} - 9\rho \rho_{(1)} \rho_{(2)} + 12\rho_{(1)}^3$$
.

As a side note, for trig-aesthetic curves (Eq. 4) we have

$$\hat{c}^2 = \frac{3\rho^5 - 2\rho^3}{\rho_{(2)}},\tag{19}$$

and inserting this in the differential equation form (10) with $a=0,\,b=1$ and $c=1/\hat{c}$, we arrive at the invariant

$$\rho_{(2)}(\rho^3 - \rho) + \rho_{(1)}^2(2 - 3\rho^2),$$
(20)

depending only on ρ , $\rho_{(1)}$ and $\rho_{(2)}$. An even simpler expression uses the derivatives of curvatures:

$$\kappa \kappa'^2 + \kappa''(1 - \kappa^2). \tag{21}$$

3.4. Plotting

The Cartesian coordinates of the curves can be given by integrating the cosine and sine of the tangent angle. Assuming that the starting point is at the origin, and the starting angle is 0, we arrive at the (x, y) coordinates

$$\left(\int_0^s \cos\left(as + \frac{b}{c}\sin(cs)\right) ds, \int_0^s \sin\left(as + \frac{b}{c}\sin(cs)\right) ds\right),\tag{22}$$

which is, however, a non-trivial integral. Lehr cites Nielsen⁶ to have converted such 'Lommel-integrals' to the solution of differential equations, and mentions their connection to Bessel functions, but in the end these did not provide a solution. Still, the dissertation contains many pages of exquisitely drawn curves (see Fig. 5) – how were these created?

Lehr plotted the integrands and used a *planimeter* (a mechanical tool for measuring the area inside a closed curve) to compute the integrals. Computations were carried out with the help of a *calculator* and a *slide-rule*. (See also Fig. 6.)

3.5. Analysis of subfamilies

In this section we will look at the characteristics of subfamilies. The classification is based on the relation between a and b, with a = b constituting the base form.



(a) Planimeter



(b) Mechanical calculator



Figure 6: Tools of the trade made in Germany in the 1930s.

3.5.1. a = b

See Figure 5a (No. 15–24) for some examples. As discussed before, these curves have no inflections, just flat points, lying on a circle of radius $x_1/\sin\theta_1$. The remaining vertices are on another circle (concentric with the first) with radius $x_1 \cot\theta_1 + y_1$. These circles degenerate to a pair of parallel lines when $\theta_1 = k\pi$ (e.g. No. 24). In this case a single period of the curve takes k full turns.

The curve is closed when θ_1 is a rational multiple of π , otherwise it goes on infinitely (e.g. No. 21). When $\theta_1 = (m + \frac{v}{n})\pi$, with v and n relative prime and v < n, the shape is 'n-gonal', and makes $\mu = mn + v$ full turns, so e.g. for No. 16

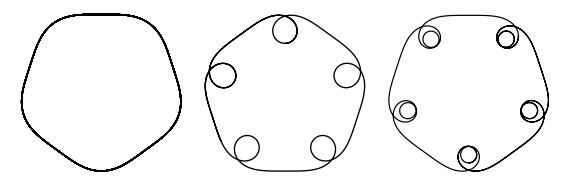


Figure 7: Appearing loops with a = b ($\theta_1 = \frac{\pi}{5}, \frac{6\pi}{5}, \frac{11\pi}{5}$).

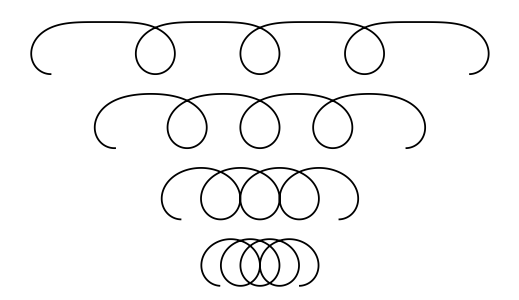


Figure 8: Shrinking spring with $\theta_1 = \pi \left(\frac{a}{b} = 1, \frac{4}{3}, \frac{15}{7}, \frac{19}{5} \right)$.

n = 3, $\mu = 4$. As m grows, more and more extra loops appear, see Figure 7, and also Appendix A.

3.5.2. a > b

We will start from the base form a=b and start to increase the $\frac{a}{b}$ ratio to see how the curve reacts. For example with $\theta_1=\frac{\pi}{2}$, we get ellipse-like closed curves (No. 25–27 in Fig. 5a). There are two dotted ellipses in each of the figures: one has the same curvatures at the vertices, and the other has matching vertices (lying very close to the curve). As $\frac{a}{b}$ increases ($\frac{4}{3}$, 2 and 4 in these three figures) the curve more and more approaches the circle.

In the case of $\theta_1 = \pi$ the base case is a series of loops, and increasing $\frac{a}{b}$ pushes them closer together, thereby touching and intersecting each other, see Figure 8. Once again, the curve approaches a circle when $\frac{a}{b}$ goes to infinity.

In general, modifying θ_1 changes the shape according to the base form, while increasing $\frac{a}{b}$ makes the loops more circle-like and thus pushes them closer together.

3.5.3. *a* < *b*

As this is a very versatile part of the family, we divide it further in our analysis.

3.5.3.1. $\theta_1 = 0$ (a = 0). Let us first look at the subgroup $\theta_1 = 0$, which will serve as a basis for understanding the other forms.

In this case it would suffice to look at the $s \in [0, \frac{\pi}{2c}]$ interval because of its symmetry. The inflection point is at the center, i.e., $\bar{s} = \frac{\pi}{2c}$, and its tangent angle there is given by $\bar{\theta} = \frac{b}{c}$. From the boundary condition $\kappa_0 = a + b = 1$ we know that b = 1, so this class is the same as the trig-aesthetic



Figure 9: Lemniscate with loops ($\theta_1 = 0$, $\bar{\theta} \approx 5.5201$).

curves, and $\bar{\theta} = \hat{c}$. Several examples are shown in Figure 1 with the associated shape parameters \hat{c} .

When $\bar{\theta} < \frac{\pi}{2}$, the curve looks like the wave

$$y = \rho_0 \tan^2 \bar{\theta} \cdot \left(1 - \cos \left(\frac{\cot \bar{\theta}}{\rho_0} x \right) \right),$$
 (23)

which has the same vertex curvatures and inflectional tangent, but at the inflection point the wave curve has larger (x,y) coordinates and arc length than our curve, so both its amplitude and wavelength is larger. These deviations get larger and larger as $\bar{\theta}$ approaches $\frac{\pi}{2}$.

When $\bar{\theta}$ grows over $\frac{\pi}{2}$, the loops get more and more circular and more closely packed, first touching and then intersecting each other. First a loop touches the next one, then, for a larger $\bar{\theta}$ value, the one adjacent to that, and so on; in the end it simultaneously touches *all* other loops and becomes a closed curve when $\bar{\theta} \approx 2.4048$, the first zero of the Bessel function of the first kind J_0 . Its shape is similar to that of Bernoulli's lemniscate, although the latter has $\bar{\theta} = \frac{3\pi}{4} \approx 2.3562$ and is slightly more elongated.

As $\bar{\theta}$ increases until π , the curve goes through the same process, but in the reverse order, touching and intersecting loops recede until they are separated, and we again get a wave-like form, but now there is an extra loop at the vertices.

For $\pi \leq \bar{\theta} \leq 2\pi$, the wave contracts and expands in the same way as before, except for the extra loops. The closed curve is obtained at $\bar{\theta} \approx 5.5201$, which is the second zero of J_0 (see Fig. 9). As one can imagine, the same things happen for $2\pi \leq \bar{\theta} \leq 3\pi$ etc., just with more extra loops. Note that the zeros of J_0 approach $\frac{3\pi}{4} + (n-1)\pi$, so the series of closed curves approaches Bernoulli's lemniscate.

In general we can also state that for $\bar{\theta} \leq \pi$ the curve resembles the *elastica*, see details in Section 3.6.

3.5.3.2. $\theta_1 = \frac{\pi}{2} \ (a = \frac{c}{2})$. We start from the base form a = b, when the excess angle ϕ is 0, and start to increase ϕ (by decreasing a and c, and increasing b). The curve starts to narrow, taking on a biscuit-like shape, until its sides touch, and then intersect each other. Then we get back the base form rotated sideways, with two extra loops, see the top of Figure 10. From here on, the same process is repeated, creating two new loops, and so on.

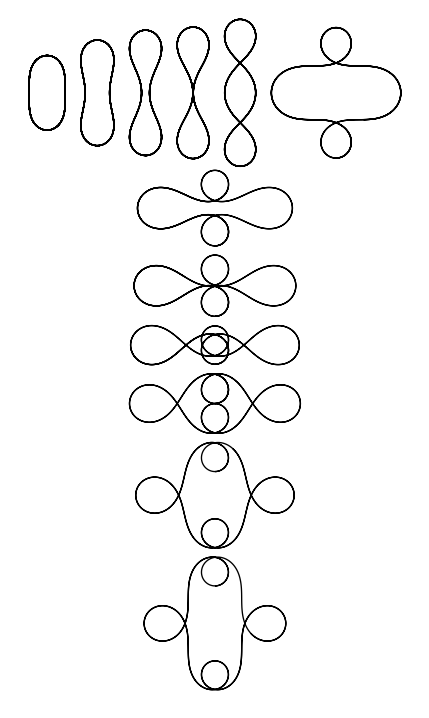


Figure 10: The $\theta_1 = \frac{\pi}{2}$ family with growing ϕ value.



Figure 11: The $\theta_1 = \pi$ family with growing ϕ value.

3.5.3.3. $\theta_1 = \pi$ (a = c). Starting from the base form a = b ($\phi = 0$), the curve contracts and then expands as ϕ is increased, exactly like in the $\theta_1 = 0$ case, except for the extra loop that is already present in the base form. See also Figure 11 showing the contraction phase.

3.5.3.4. Generalization. The base form is defined by $\theta_1.$ Increasing φ converts flat points into two inflection points and an arc with negative curvature between them, appearing as indentations or bulges. As these grow larger, the curve seems to contract, and individual parts of the curve touch, until eventually all vertices of a given type fall into the center of the curve. Then these vertices move farther away from the center, and vertices with the other curvature start to approach it. The process repeats as φ increases by $\pi.$

3.6. Comparison with elastic curves

The subfamily a=0 is very similar to the *elastica* family studied by Jacob Bernoulli and Euler. Since this has recently been also emphasized in a paper on trig-aesthetic curves, we will show the correspondences in notation.

 $[\]P$ The tangent was not squared in the original, but that would not satisfy the constraints given in the text.

3.6.1. Elastica equations

Elastic curves have many definitions, based on pendulums, or the minimization of bending energy while retaining arc length. The one used by Lehr (following Bernoulli) is that the curvature at a given point is proportional to the distance from the line of force. Mathematically, taking the x axis as the line, and the proportional factor $-m^2$, this is described by the equation

$$\kappa = -m^2 y. \tag{24}$$

Since $d\theta/ds = \kappa$ and $dy/ds = \sin \theta$, we obtain

$$\left(\frac{\mathrm{d}^2 y}{\mathrm{d}s^2}\right)^2 = \left(1 - \left(\frac{\mathrm{d}y}{\mathrm{d}s}\right)^2\right) m^4 y^2. \tag{25}$$

Now using v = dy/ds, we have

$$\left(v\frac{dv}{dy}\right)^2 = (1 - v^2)m^4y^2,$$
 (26)

and taking square root

$$\frac{\mathrm{d}v}{\mathrm{d}v} = \pm \frac{\sqrt{1 - v^2} m^2 y}{v}.$$
 (27)

Separating the variables and integrating, we get

$$\int \frac{v}{\sqrt{1 - v^2}} \, \mathrm{d}v = \pm \int m^2 y \, \mathrm{d}y. \tag{28}$$

With $u = 1 - v^2$ (i.e., $v dv = -\frac{1}{2} du$), this leads to

$$\int -\frac{1}{2\sqrt{u}} \, \mathrm{d}u = \pm \frac{m^2 y^2}{2} + C. \tag{29}$$

The integral of the left-hand side is just $-\sqrt{u} = -\sqrt{1 - v^2}$ (plus an integration constant absorbed by C), so squaring both sides we obtain

$$1 - v^2 = \left(\frac{m^2 y^2}{2} + C\right)^2,\tag{30}$$

where C also absorbs the \pm sign. Finally this gives us

$$\frac{\mathrm{d}y}{\mathrm{d}s} = \sqrt{1 - \left(\frac{m^2 y^2}{2} + C\right)^2}.\tag{31}$$

(Lehr jumps directly from Eq. (25) to Eq. (31), as the intermediate steps are straightforward...)

The above leads to an elliptic integral form of arc length:

$$s = \int_{y_0}^{x_y} \frac{\mathrm{d}y}{\sqrt{1 - \left(\frac{m^2 y^2}{2} + C\right)^2}} \tag{32}$$

The intrinsic equation is then given by the use of the Jacobi elliptic function cn:

$$\kappa = m\sqrt{2(1-C)}\operatorname{cn}(ms). \tag{33}$$

Once again, this step is not trivial. Let us first formulate the differential equation for the elastic curve. Deriving Eq. (24)

$$\frac{\mathrm{d}^2 \theta}{\mathrm{d}s^2} = \frac{\mathrm{d}\kappa}{\mathrm{d}s} = -m^2 \frac{\mathrm{d}y}{\mathrm{d}s} = -m^2 \sin \theta,\tag{34}$$

so

$$\frac{\mathrm{d}^2}{\mathrm{d}s^2}\Theta(s) + m^2\sin\Theta(s) = 0. \tag{35}$$

Multiplying by $d\theta/ds$ and integrating it results in

$$\frac{1}{2}\kappa^2 - m^2\cos\theta = E,\tag{36}$$

where E is the integration constant. Its value is not arbitrary, however: from Eq. (31) we know that

$$\sqrt{1-\cos^2\theta} = \sin\theta = \frac{dy}{ds} = \sqrt{1-\left(\frac{m^2y^2}{2}+C\right)^2},$$
 (37)

so $\cos \theta = \frac{m^2 y^2}{2} + C$, and inserting it into Eq. (36) leads to

$$E = \frac{1}{2}(-m^2y)^2 - m^2\left(\frac{m^2y^2}{2} + C\right) = -m^2C,$$
 (38)

so once again using Eq. (36) we obtain

$$\frac{\mathrm{d}\theta}{\mathrm{d}s} = \kappa = \pm m\sqrt{2(\cos\theta - C)}.\tag{39}$$

We can omit the sign as it will be absorbed by a constant later on. Separating the variables and integrating, assuming $s_0 = 0$, results in

$$s = \frac{1}{m\sqrt{2}} \int \frac{\mathrm{d}\theta}{\sqrt{\cos\theta - C}}.\tag{40}$$

For convenience we change the variable to $\hat{\theta} = \frac{\theta}{2}$, using the fact that $\cos \theta = 1 - 2\sin^2 \frac{\theta}{2}$:

$$s = \frac{\sqrt{2}}{m\sqrt{1-C}} \int \frac{\mathrm{d}\hat{\theta}}{\sqrt{1-\frac{2}{1-C}\sin^2\hat{\theta}}} \tag{41}$$

$$=\frac{\sqrt{2}}{m\sqrt{1-C}}\cdot F\left(\frac{\theta}{2},\frac{2}{1-C}\right),\tag{42}$$

where F is the incomplete elliptic integral of the first kind. Here $k^2 = \frac{2}{1-C}$ is called the *parameter*, and k is the *modulus*. Denoting the value of the incomplete integral as u, we have

$$u = ms\sqrt{\frac{1-C}{2}} = \frac{ms}{k},\tag{43}$$

so $\frac{\theta}{2} = \text{am}(u, k^2)$, the Jacobi amplitude. This means that

$$\cos \theta - C = 1 - 2\sin^2 \frac{\theta}{2} - C = 1 - C - 2\sin^2(u, k^2)$$
 (44)

$$= 2\left(\frac{1}{k^2} - \operatorname{sn}^2(u, k^2)\right),\tag{45}$$

so

$$\kappa = 2m\sqrt{\frac{1}{k^2} - \text{sn}^2(u, k^2)}.$$
 (46)

Since $dn^2(u, k^2) = 1 - k^2 sn^2(u, k^2)$, we arrive at

$$\kappa = \frac{2m}{k} dn(u, k^2) = m\sqrt{2(1-C)} dn(u, k^2).$$
(47)

Finally, using the relationship $dn(u, k^2) = cn(uk, 1/k^2)$, we at last obtain the expression

$$\kappa = m\sqrt{2(1-C)}\operatorname{cn}\left(ms, \frac{1-C}{2}\right). \tag{48}$$

We see that in this form the modulus is $\sqrt{\frac{1-C}{2}}$. The m parameter is essentially scaling the curve, and only C controls the shape. In the differential equation form (Eq. 35), when used with fixed boundary conditions $\theta(0) = 0$ and $\kappa(0) = 1$, the shape is controlled by $\lambda := m^2$.

By squaring Eq. (39) we get

$$\kappa^2 = 2m^2(\cos\theta - C). \tag{49}$$

which for the above mentioned boundary conditions gives

$$1 = 2m^2(1 - C),$$

leading to the relationship

$$\lambda = m^2 = \frac{1}{2(1 - C)}. (50)$$

3.6.2. Comparison

Note that the \hat{c} parameter of trig-aesthetic curves is the same as $\bar{\theta}$, when the latter is real. Refer to Figure 12 for a visual comparison.

Lehr divides the family into classes based on the value of the C integration constant, each exhibiting a distinct shape type:

- C = 1 ($\lambda = \infty$, $\bar{\theta} = 0$): both curves degenerate to a line.
- 0 < C < 1 $(\frac{1}{2} < \lambda < \infty, 0 < \bar{\theta} < \frac{\pi}{2})$: both are similar to sine waves; vertex curvature is ± 1 for both, but the amplitude and wavelength is smaller for trig-aesthetic curves.
- C = 0 (λ = ½, θ = π/2): Lehr states that this is the only elastic curve that is also a Ribaucour curve (with factor 2), i.e., the radius of curvature is proportional to the normal directional distance to a given line. This seems not to be the case: here the curvature (and not the *radius* of curvature) is proportional to the normal distance.
- -1 < C < 0 $(\frac{1}{4} < \lambda < \frac{1}{2}, \frac{\pi}{2} < \bar{\theta} < \pi)$: we further divide into 3 cases below
 - $\bar{x} > 0$: both curves touch, contract and intersect themselves, the difference in amplitude is more and more visible.
 - $\bar{x}=0$: Bernoulli's lemniscate is an intermediate form between the two, as can be seen from the values of $\bar{\theta}$ (elastica: $\approx 130^{\circ}42'$, lemniscate: 135° , trig-aesthetic: $\approx 137^{\circ}47'13''$).
 - \bar{x} < 0: the loops start to separate, much faster for the elastica than for trig-aesthetic curves.

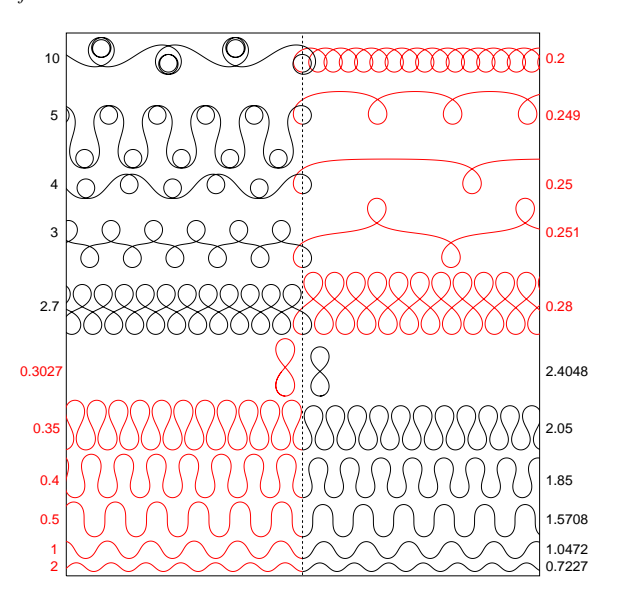


Figure 12: Comparison of trig-aesthetic curves (black) and elastica (red). The associated numbers show the values of $\hat{c} = \bar{\theta} = \frac{1}{c}$ for the former, and of λ for the latter, with the boundary conditions $\theta(0) = 0$ and $\kappa(0) = 1$. For rows where $\lambda > \frac{1}{4}$, trig-aesthetic curves were selected based on visual similarity, but not necessarily with the same $\bar{\theta}$ value; the other examples are included to illustrate a variety of forms.

• C = -1 ($\lambda = \frac{1}{4}$, $\bar{\theta} = \pi$): from here on, the two curves have no connection. In this special case the elastica has the closed form

$$\left(-\frac{2}{m}\sin\frac{\theta}{2} + \frac{1}{m}\ln\tan\left(\frac{\theta}{4} + \frac{\pi}{4}\right), \frac{2}{m}\left(1 - \cos\frac{\theta}{2}\right)\right). \tag{51}$$

- $-\infty < C < -1$ ($0 < \lambda < \frac{1}{4}$, $\bar{\theta}$ imaginary): the elastica takes on an ever-contracting spring-like form, while the trig-aesthetic curve ($\pi < \hat{c} < \infty$) goes through contractions and expansions as explained in Section 3.5.
- $C = -\infty$ ($\lambda = 0$, $\bar{\theta}$ imaginary): corresponds to the case $\hat{c} = \infty$; both curves are circles.

3.7. Space curves

As a generalization to 3D space, we can add a constraint on the radius of torsion τ , similarly to Eq. (5):

$$\frac{1}{\tau} = \alpha + \beta \cos(\gamma s + \delta). \tag{52}$$

But the Frenet equations can only be integrated easily when $\delta=0,\,c=\gamma$, and $\alpha\beta-ab=0$, i.e.,

$$\frac{1}{\rho} = a + b\cos(cs), \qquad \frac{1}{\tau} = \alpha + \frac{ab}{\alpha}\cos(cs).$$
 (53)

^{||} With some corrections.

These are all helices that can be constructed on a cylinder whose normal section is a curve of Eq. (5).

Since this line of generalization does not seem to be very fruitful, Lehr turns to curves defined on the sphere with geodesic curvature

$$\kappa_g = \frac{1}{\rho_g} = a + b\cos(cs). \tag{54}$$

Since $\kappa^2 = \kappa_g^2 + \kappa_n^2$, and the normal curvature κ_n on a sphere of radius *R* is $\frac{1}{R}$, we have

$$\frac{1}{\rho} = \sqrt{(a+b\cos(cs))^2 + \frac{1}{R^2}}, \quad \frac{1}{\tau} = \frac{Rbc\sin(cs)}{R^2(a+b\cos(cs))^2 + 1}.$$
(55)

If *R* goes to infinity, the torsion approaches zero and we get back our original curves. Otherwise this leads to a complex Riccati differential equation, but we can make some general remarks

- The curves are periodic with period $\frac{2\pi}{c}$.
- The curvature is always positive, and maximal at the endpoints.
- The minimal value of (ordinary or geodesic) curvature is at the midpoint $s = \frac{\pi}{c}$, where the torsion is zero.
- The geodesic curvature becomes zero when $\cos(cs) = -\frac{a}{b}$ (occurs for two values when a < b, symmetric to the midpoint).

For easier analysis and plotting, Lehr uses stereographic projection onto the equatorial plane (see Fig. 5b). For a spherical point (x, y, z) the projection is

$$(\xi, \eta) = \frac{R}{R - \tau}(x, y), \tag{56}$$

while the inverse projection is

$$(x, y, z) = \frac{1}{\xi^2 + \eta^2 + R^2} (2R^2 \xi, 2R^2 \eta, R(\xi^2 + \eta^2 - R^2)). \tag{57}$$

A circle around a projected point (ξ_0,η_0) with radius ρ_0 is also a circle on the sphere in the plane

$$Ax + By + Cz + D = 0 ag{58}$$

with A:B:C:D being**

$$2R\xi_0: 2R\eta_0: \xi_0^2 + \eta_0^2 - \rho_0^2 - R^2: -R(\xi_0^2 + \eta_0^2 - \rho_0^2 + R^2).$$
(59)

Then the radius of the 3D circle ρ depends on the distance δ of the plane from the center ($\rho^2 = R^2 - \delta^2$). Consequently:

$$\rho^2 = \frac{4R^4\rho_0^2}{(\xi_0^2 + \eta_0^2 - \rho_0^2 - R^2)^2 + 4R^2(\xi_0^2 + \eta_0^2)}.$$
 (60)

If we now look at a circle going through (ξ^*, η^*) with tangent angle t^* (measured from the positive ξ axis), we get

$$\xi_0 = \xi^* \pm \rho_0 \sin t^*, \qquad \eta_0 = \eta^* \mp \rho_0 \cos t^*, \qquad (61)$$

so if we introduce $d^2 = \xi^{*2} + \eta^{*2}$ for the squared distance of the point from the origin, and $c = \pm \xi^* \sin t^* \mp \eta^* \cos t^*$ for the signed distance of the origin from the tangent line, we arrive at

$$\rho^2 = \frac{4R^4 \rho_0^2}{(d^2 + 2\rho_0 c - R^2)^2 + 4R^2(d^2 + \rho_0^2 + 2\rho_0 c)},$$
 (62)

and then

$$\rho_0 = \frac{(d^2 + R^2)\rho}{2(R\delta - c\rho)} = \frac{d^2 + R^2}{2(e - c)},$$
(63)

with $e = \frac{R\delta}{\rho}$.

For a spherical curve with known geodesic curvature, the curvature circle is obtained by intersecting the sphere with the osculating plane. From this we can compute the curvature circle in the plane, whose radius gives the radius of curvature for the projected curve (note that with ρ being the radius of curvature, we have $e = \frac{R^2}{\rho_g}$). Now we have all information to plot the 2D image of the curve.

Let us take example No. 31 in Figure 5a (a trig-aesthetic curve with $\hat{c} = \frac{11}{14}$), and create its geodesic curvature version on a large sphere. The resulting curve is very similar (see Fig. 5b, No. 89, $\rho_g(0)/R = 0.4$). As we reduce the sphere's radius, the vertices approach each other, and then separate again (No. 90–94, $\rho_g(0)/R = 1, 1.2, 1.37, 1.4, 2$). The curve can also close on itself, as shown in No. 95 ($\rho_g(0)/R = 2.94$). As R approaches 0, the curve approximates a great circle of the sphere.

Conclusion

Eduard Lehr described the curve family defined by Eq. (5), investigating the parameters' effect on its different shapes, including the *base forms* and what are now called *trigaesthetic curves*. Notes on derived curves (evolute, offset and involute) were supplied. A comparison to Euler's *elastica* was also included, as well as preliminary work on generalization to space curves, particularly to spherical curves.

In this work we have aimed to extract the most interesting parts from Lehr's dissertation, and also supplemented it in several places, notably on the derivation of the elastic curve, and by the addition of a figure comparing it to trig-aesthetic curves. Several errors in the equations were corrected, and some biographical background on Lehr was also included for completeness.

Acknowledgements

This project has been supported by the Hungarian Scientific Research Fund (OTKA, No. 145970). The author would like to thank the Max-Planck-Gymnasium München, the Bavarian State Archives, the Military Archives of the Federal Archives of Germany, and the Library and Archives of the Technical University of Munich for providing biographical data on Eduard Lehr.

^{**} The equations from here on contained errors in the original.

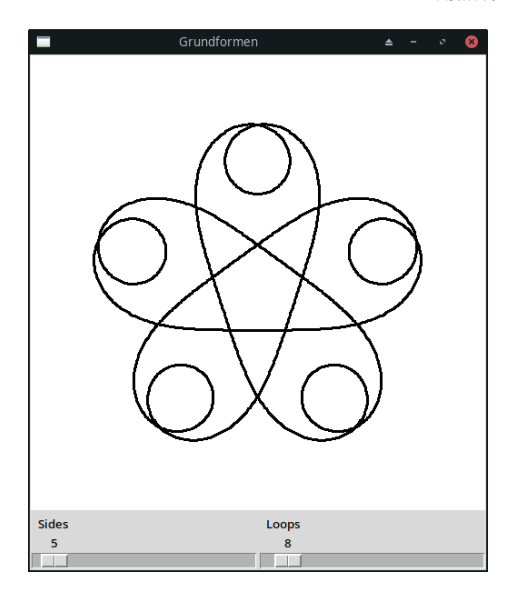


Figure 13: Applet for experimenting with base forms.

References

- Elsa Abbena, Simon Salamon, and Alfred Gray. Modern Differential Geometry of Curves and Surfaces with Mathematica. Chapman and Hall/CRC, 3rd edition, 2017.
- Ernesto Cesàro. Lezioni di geometria intrinseca. Naples, 1896.
- Eduard Lehr. Über die Kurven, deren Krümmung eine periodische Funktion des Bogens ist. PhD thesis, Technische Hochschule München. 1932.
- Luna B. Leopold and Walter Basil Langbein. River meanders. Scientific American, 214(6):60–73, 1966.
- Kenjiro T. Miura and R. U. Gobithaasan. Log-aesthetic curves and similarity geometry. *International Journal of Automation Technology*, 18:591–602, 2024.
- Niels Nielsen. Handbuch der Theorie der Cylinderfunktionen.
 B. G. Teubner, 1904.
- Péter Salvi. Generalized catenaries and trig-aesthetic curves. Computer-Aided Design and Applications, 23(1):56–67, 2026.
- Stephen Wolfram. A New Kind of Science. Wolfram Media, 2002.

Appendix A: Applet for exploring base forms

The TCL/TK applet in Figure 13 is a convenient tool for plotting different base forms; it can also be easily modified to investigate other curves. Here a=b=1 and $c=n_{\rm sides}/n_{\rm loops}=n/\mu$. The source code is shown in Figure 14, and is embedded in the PDF version of this document.

```
lassign {500 3 200} size lineWidth resolution; # params
 lassign {5 8} sides loops
wm title
                     "Grundfor
canvas .canvas -width $size -height $size -bg white
scale .f.sides -variable sides -from 1 -to 100
-label Sides -orient horizontal -command redraw scale .f.loops -variable loops -from 1 -to 100
-label Loops -orient horizontal -command redraw
pack .f.sides .f.loops -side left -expand 1 -fill x
pack .canvas .f -fill x
       redraw args {
    global resolution loops size lineWidth
        .canvas delete all
       .canvas delete all
set res [expr {$resolution*$loops}]
set smax [expr {2*$loops*acos(-1)}]
lassign {{0 0} {0 0} {0 0} p bbmin bbmax s1
set points [list $p]
for {set i 0} {$i < $res} {incr i} {
    set s [expr {$smax*$i/($res-1.0)}]
    set d [list [integrate fx $s1 $s]
    [integrate fx $s1 $s]
                                    [integrate fy $s1 $s]]
               set p [add $p $d]
               set bbmin [vmin $p $bbmin]
set bbmax [vmax $p $bbmax]
               lappend points $p
               set s1 $s
       set scale [expr {$size/[distance $bbmin $bbmax]}]
set center [mul [add $bbmin $bbmax] -0.5]
set offset [list [expr {$size/2}] [expr {$size/2}]]
set coords {}
foreach p $points {
               lappend coords {*}[add [mul [add $p $center]
                                                                 $scale]
                                                        $offset]
        .canvas create line $coords -width $lineWidth
}
proc vmin {u v} {
    list [expr {min([lindex $u 0],[lindex $v 0])}]
        [expr {min([lindex $u 1],[lindex $v 1])}]
proc vmax {u v} {
    list [expr {max([lindex $u 0],[lindex $v 0])}]
        [expr {max([lindex $u 1],[lindex $v 1])}]
proc add {u v} {
    list [expr {[lindex $u 0]+[lindex $v 0]}]
        [expr {[lindex $u 1]+[lindex $v 1]}]
proc norm u {expr {sqrt([dot $u $u])}}
proc distance {p q} {norm [sub $p $q]}
proc theta {s} {
       global sides loops
set c [expr {($sides+0.0)/$loops}]
expr {$s+1/$c*sin($c*$s)}
proc fx {s} {expr {cos([theta $s])}}
proc fy {s} {expr {-sin([theta $s])}}
proc integrate {f a b} {
        set x {-0.906179845937 -0.538469310107 0
                      0.538469310107 0.906179845937}
       set m [expr {($a+$b)/2}]
for {set i 0} {$i < 5} {incr i} {
    set xi [expr {($b-$a)/2*[lindex $x $i]+$m}]
    set sum [expr {$sum+[lindex $w $i]*[$f $xi]}]</pre>
       expr {$sum*($b-$a)/2}
redraw
```

Figure 14: TCL/TK source for the applet in Fig. 13.